

Energetics, Structure, and Electron Detachment Spectra of Calcium and Zinc Neutral and Anion Clusters: A Density Functional Theory Study

Yafei Dai and Estela Blaisten-Barojas*

Computational Materials Science Center and Department of Computational and Data Sciences, George Mason University, Fairfax, Virginia 22030

Received: April 18, 2008; Revised Manuscript Received: September 5, 2008

A hybrid density functional approach with very large basis sets was used for studying Ca₂ through Ca₁₉ and Zn₃ through Zn₁₁ neutral clusters and their cluster anions. Energetics, structure, and vibrational analysis of all these neutral clusters and cluster anions are reported. The calculated electron affinities are in excellent agreement with experiment displaying a characteristic kink at Ca₁₀ and Zn₁₀. This kink occurs because the 10-atom neutral cluster is very stable whereas the cluster anion is not. Additionally, the electron detachment binding energies (BEs) up to Ca₆⁻ and Zn₆⁻ were identified by analyzing the ground and excited states of the cluster anions and of their corresponding size neutral clusters. The theoretical BE is in very good agreement with experiment for both calcium and zinc cluster anions. The three main peaks in the spectrum correspond to BEs from the ground state of the cluster anion (doublet) to the ground state of the neutral cluster (singlet) and to the first triplet and quintet excited states of the neutral cluster. The calculated energy gap from the lowest BE peak to the second peak is in excellent agreement with experiment. The calculation reproduces very well the energy gap observed in Ca₄⁻ and Zn₄⁻, which is larger than those for other sizes and is indicative of the strong stability of the anion and neutral tetramers.

1. Introduction

Calcium is the fifth most abundant element on the earth and plays an essential role for living organisms, compounds, and mechanisms. Metal clusters span the gap between the atomic and the bulk length scales, and their study furthers the understanding of the electronic behavior of metals at the nanoscale.^{1–3} Calcium clusters have attracted the interest of scientists in the past few years such that energetics, structure, vibrational frequencies, and thermodynamic properties have been studied in detail from various perspectives.^{4–7} On the other hand, calcium cluster anions have received much less attention, especially concerning their electronic properties, which are fundamental for the theoretical description of photoelectron detachment spectroscopy.⁸

Zinc is the fourth most common metal in use, trailing only to iron, aluminum, and copper in annual production. Bulk bonding features of group IIB elements are transient from van der Waals to covalent and finally to metallic, which make these metals interesting from the perspective of subnanometer scale systems. Among these elements Hg clusters are the most extensively studied.^{9–15} To a lesser extent, Zn clusters have also been studied, both experimentally^{8,16,17} and theoretically.^{18–20} However, the theoretical studies address neutral zinc clusters only, and little is known about the zinc cluster anions.

Older experimental photoelectron spectroscopy results for small clusters of elements in the fourth row of the periodic table comprise K,²¹ Ti,²² and Co.²³ Calcium and zinc are two elements in the fourth row of the periodic table for which experiments on the electron affinity⁸ and the electron detachment spectra^{8,17} have been reported more recently. It is therefore important and feasible to theoretically study the underlying electronic states involved in the experimental process. In this work we perform an exhaustive all-electron study within hybrid density functional

theory (DFT) of the ground state of neutral clusters and cluster anions for sizes up to Ca₁₉ and up to Zn₁₁. Such study gives insight on the energetics, structure, and vibrational analysis and allows for comparison of the electron affinity to the available experimental results. Additionally, the excited states of the smaller neutral clusters and their cluster anions up to $n = 6$ were studied for both calcium and zinc. Knowledge of the excited states of both neutrals and anions allows for molecular identification of the experimental peaks appearing in the electron detachment energy spectrum. The computational task of finding the excited states of larger than 6-atom clusters is beyond our current computational power and is not attempted in this paper.

This paper is organized as follows. Section 2 contains the theoretical methodology, the energetics of the calcium and zinc neutral and anion clusters, and provides a comparison of experimental and theoretical results of the electron affinities up to Ca₁₉ and Zn₁₁. Sections 3 and 4 give details on the excited states of the neutral and negatively charged clusters up to Ca₆ and Zn₆ that enter in the identification of the electron detachment spectra and provide comparison with experimental results. This paper is concluded with closing remarks in section 5.

2. Energetics of Ca_n ($n = 2–19$) and Zn_n ($n = 3–11$) Neutral and Anion Clusters

All-electron calculations on calcium and zinc neutral and anion clusters were carried out within the hybrid Becke density functional theory (DFT), B3PW91, which contains the Perdew–Wang local and nonlocal correlation functionals.^{24,25} The 6-311G(d) triple valence basis set^{27,28} with s, p, d polarization was used throughout this paper. However, for the small Ca clusters up to $n = 11$ and for all Zn clusters, the basis set was expanded with d-diffuse functions 6-311+G(d). As expected for calcium, diffuse d-functions decrease marginally the energy of the Ca cluster anions because d-orbital momentum symmetry

* Corresponding author, blaisten@gmu.edu.

TABLE 1: Electronic Energies (E) with Symmetry and Ground-State Identification of Ca_2 through Ca_{19} Anion and Neutral Clusters and Their Electron Affinity (EA)

| Ca_n | neutral | | | anion | | | EA (eV) | |
|---------------|----------------|----------------|------------|------------|----------------|----------------|------------|------------|
| | sym | state | E (eV) | | sym | state | E (eV) | |
| | | | 6-311 g(d) | 6-311+g(d) | | | 6-311 g(d) | 6-311+g(d) |
| 2 | $D_{\infty h}$ | $^1\Sigma_g^+$ | -0.1468 | -0.1478 | $D_{\infty h}$ | $^2\Pi_u$ | -0.6417 | 0.4934 |
| 3 | D_{3h} | $^1A_1'$ | -0.6612 | -0.6647 | D_{3h} | $^2\Sigma_g^+$ | -0.6602 | 0.5121 |
| 4 | T_d | 1A_1 | -1.7751 | -1.7836 | T_d | $^2A_1''$ | -1.5491 | 0.8862 |
| 5 | D_{3h} | 1A_1 | -2.3948 | -2.4159 | D_{3h} | $^1A_1'$ | -2.7160 | 0.9468 |
| 6 | C_{2v} | 1A_1 | -3.0826 | -3.1112 | C_{2v} | 2A_2 | -3.3957 | 1.0100 |
| 7 | D_{5h} | $^1A_1'$ | -4.3597 | -4.4066 | C_{2v} | 2A_2 | -4.2415 | 1.1612 |
| 8 | C_s | $^1A'$ | -5.1021 | -5.1603 | C_s | $^2A_2''$ | -4.2667 | 1.1580 |
| 9 | C_1 | 1A | -6.1861 | -6.2577 | C_1 | 2A | -5.4926 | 1.1441 |
| 10 | D_{3h} | $^1A_1'$ | -7.5126 | -7.5995 | C_1 | 2A | -5.5338 | 1.1387 |
| 11 | C_1 | 1A | -8.2656 | -8.3851 | C_1 | 2A | -6.4305 | 1.2829 |
| 12 | C_1 | 1A | -9.0720 | | C_1 | 2A_2 | -7.5249 | 1.2753 |
| 13 | C_1 | 1A | -10.2689 | | C_1 | 2A | -8.5409 | 1.3389 |
| 14 | C_1 | 1A | -11.3565 | | C_1 | 2A | -9.4992 | 1.3065 |
| 15 | C_1 | 1A | -12.0087 | | C_1 | 2A_2 | -10.4271 | 1.0414 |
| 16 | C_1 | 1A | -13.4332 | | C_1 | 2A | -11.7244 | 1.0263 |
| 17 | C_1 | 1A | -15.0069 | | C_1 | 2A | -12.8522 | 1.2376 |
| 18 | C_1 | 1A | -16.1052 | | C_1 | 2A | -13.5546 | 1.2186 |
| 19 | D_{5h} | $^1A'$ | -17.6005 | | D_{5h} | 2A_2 | -14.8909 | 1.4621 |

is absent from the occupied states. On the other hand for Zn clusters, d-diffuse functions are significantly effective in reducing the energy of the neutrals and anions. All self-consistent energy results are accurate up to eight decimals and only the first three or four decimals are reported in the tables. The Gaussian 2003²⁹ package was used throughout this paper.

For studying theoretically the electron affinity (EA) and comparing with EA experiments,⁸ the ground state of the cluster anions Ca_2^- through Ca_{19}^- and the ground state of the corresponding neutral clusters Ca_2 through Ca_{19} are studied in this section. A similar study is performed for Zn_3^- through Zn_{11}^- . On the basis of this information, the EA is calculated as the difference between the total energies of the ground state of the neutral and anion clusters taking into account the zero point energy ϵ_0 of each state: $(E_{\text{TOTAL}} + \epsilon_0)_{\text{neutral}} - (E_{\text{TOTAL}} + \epsilon_0)_{\text{anion}}$.

Results of the ground-state energy E , symmetry group, and electronic state identification for neutral and anion calcium clusters containing 2–19 atoms are given in Table 1, where all total energies are relative to the energy of separated neutral calcium atoms. The total energies of the neutral calcium atom and its anion are -677.50978286 au, -677.50976233 au with 6-311G(d), and -677.50981264 au, -677.51303514 au with 6-311+G(d), respectively. The total energies of the neutral and anion zinc atoms with 6-311+G(d) are -1779.30681367 au and -1779.27185139 au, respectively. An exhaustive search for the structures of lowest energy was conducted for each cluster size adopting the following strategy. A multitude of cluster structures from previous studies^{4–7} were used as initial geometries of the geometry optimization with the purpose of finding the energy minima. This optimization was performed with the Berny algorithm and redundant internal coordinates.²⁶ Additionally, structures in Table 1 were verified to be a minimum by the calculation of the vibrational frequencies. The Berny algorithm is based on steepest descents. Therefore, in configuration space the algorithm drives the system to the minimum closest to the initial geometry. It is known that a cluster of atoms has many minima, each minimum corresponding to a stable isomer of that cluster size. Along this study, several stable isomers were identified for each cluster size, although Table 1 reports only those isomers corresponding to the minimum of lowest energy

found up-to-date. Several saddles of different orders of the energy landscape were also discovered and are not reported in this paper either. Up to $n = 11$, Table 1 shows results employing the 6-311G(d) and 6-311+G(d) basis sets. Although energies decrease up to 0.1 eV with the larger basis set, our results show that energy differences such as the EA are marginally affected by the added diffuse d-function. The effect of the diffuse d-function is important only for Ca_2^- by producing an inversion of the two lower doublet states.

Figure 1a depicts the second difference of the energy $E(n - 1) + E(n + 1) - 2E(n)$ for calcium clusters. In upcoming paragraphs this second difference is referred to as the energy stability pattern. In this energy pattern, peaks correspond to clusters that are relatively more stable than those with nearest sizes. The solid line in Figure 1a depicts data for the neutral clusters and the dashed line pertains to the cluster anions. It is readily apparent that neutral calcium clusters containing 4, 7, 10, 13, and 17 have high peaks and are therefore very stable. The energy stability pattern of the anion clusters is similar to that of the neutrals except for the peaks at $n = 9$ and 10. The anion Ca_{10}^- is less stable than Ca_9^- or Ca_{11}^- whereas the neutral Ca_{10} is very stable when compared to the neighboring size clusters.

Zinc cluster anions and neutrals containing 3–11 atoms are reported in Table 2, and their energy stability pattern is given in Figure 1b (solid line for neutrals and dashed line for cluster anions). The table summarizes the ground-state energy, symmetry, and electronic state. Energies are relative to the energy of the separated neutral atoms. Peaks in Figure 1b indicate that neutral clusters with 4, 7, and possibly 10 atoms are relatively more stable than neighboring sizes, and the same behavior is apparent for the cluster anions except for Zn_9 and Zn_{10} . Therefore in the very small cluster size regime, both Ca and Zn have similar energy stability.

The geometries of the Ca cluster anions are shown in Figure 2. The structures of neutral Ca_2 through Ca_{12} have been reported in previous work⁴ within the same DFT approach. Ca_{13} is a twinned pentagonal pyramid with one decorated face, which is 0.1163 eV more stable than the lowest of three previously reported isomers.⁴ With this new structure, the number of known

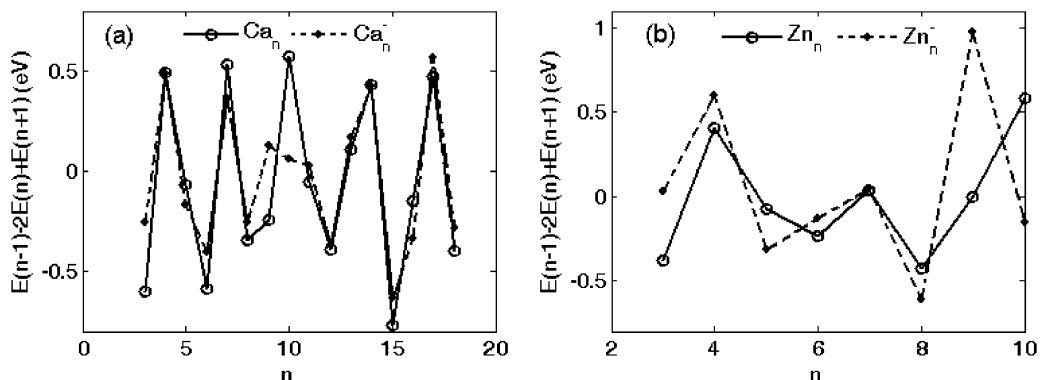


Figure 1. Stability pattern as a function of cluster size: (a) calcium; (b) zinc. Dotted lines correspond to cluster anions and full lines to neutral clusters.

TABLE 2: Electronic Energies (*E*) with Symmetry and Ground-State Identification of Zn_3 through Zn_9 Anion and Neutral Clusters and Their Electron Affinity (EA)

| Zn_n | neutral | | | anion | | | EA (eV) |
|--------|----------|----------|---------------|----------|----------|---------------|---------|
| | sym | state | <i>E</i> (eV) | sym | state | <i>E</i> (eV) | |
| 3 | D_{3h} | $^1A_1'$ | -0.1537 | D_{3h} | $^2A_1'$ | -0.6802 | 0.5173 |
| 4 | T_d | 1A_1 | -0.6662 | T_d | 2A_1 | -1.4739 | 0.8073 |
| 5 | D_{3h} | $^1A_1'$ | -0.7745 | D_{3h} | $^2A_1'$ | -1.6688 | 0.8955 |
| 6 | C_{2v} | 1A_1 | -0.9570 | C_{2v} | 2A_1 | -2.1811 | 1.2114 |
| 7 | C_1 | 1A | -1.3734 | C_1 | 2A | -2.8245 | 1.4429 |
| 8 | C_1 | 1A | -1.7555 | C_1 | 2A | -3.4199 | 1.6515 |
| 9 | C_{2v} | 1A_1 | -2.5664 | C_{2v} | 2A_1 | -4.6267 | 2.0514 |
| 10 | C_1 | 1A | -3.3758 | C_1 | 2A | -4.8540 | 1.4724 |
| 11 | C_1 | 1A | -3.5998 | C_1 | 2A | -5.1877 | 1.5766 |

stable isomers of Ca_{13} is increased to four. This new Ca_{13} was seeded with one extra atom to yield Ca_{14} . Neutral Ca_{15} through Ca_{19} are slightly distorted structures predicted at the tight-binding (TB) level.⁷ Geometry optimizations of the $n = 15$ –19 clusters were started from a variety of initial configurations, including the published structures.⁷ Results reported in Table 1 indicate that the TB structures with minor deformations that break the symmetry are the lowest in energy found to date. A commonality of the cluster anions is a slight structural distortion when compared to the neutral counterparts due to the negative charge. For example, Ca_5^- and Ca_6^- shown in Figure 2 present slightly elongated bond lengths vis-a-vis of the neutral clusters Ca_5 D_{3h} and Ca_6 C_{2v} reported in ref 4. Comparable distortions yield a less symmetric (C_{2v}) Ca_7^- instead of the D_{5h} neutral cluster.

The geometries of the Zn cluster anions are shown in Figure 3. Except for Zn_7 and Zn_8 , our optimized structures of Zn_3 through Zn_{11} are in agreement with both DFT calculations using basis sets without diffuse d-functions¹⁹ and MP2/LANL2DZ calculations.²⁰ Our Zn_7 is the same as that given in ref 19 while the structure reported in ref 20 is found to be a saddle. In the case of Zn_8 , our structure coincides with the 8b isomer of ref 19 and the other reported structures are found to be higher in energy or not stable. As already stated in ref 19, the expected comparison of DFT results to coupled-clusters (CC) results¹⁸ is reasonable for Zn clusters with $n = 4$ –6 but may not reproduce well the incipient van der Waals bonding of zinc dimers and trimers. Not all the Zn anion clusters maintain the structure of the neutrals with small distortions. As seen in Figure 3, Zn_6^- , Zn_8^- , and Zn_{10}^- have different geometries than those corresponding to the neutral clusters.

The EAs of the Ca and Zn clusters are reported in the last column of Tables 1 and 2. For calcium clusters, the EAs up to $n = 11$ were calculated with the 6-311G(d) and 6-311+G(d)

basis sets. As is clear from Table 1, the expanded basis set with diffuse functions adds minor corrections of only a couple of hundredths of an electronvolt to the EA. Figures 4a and 4b (dotted lines with triangles) are plots of the EA of calcium and zinc clusters as a function of size showing the comparison with experimental results (solid line with circles) of ref 8. The qualitative agreement for both calcium and zinc clusters is excellent. For calcium, the notorious kink at the 10-atom cluster occurs because neutral Ca_{10} is very stable (peak in Figure 1a) whereas the cluster anion Ca_{10}^- is relatively not stable (valley in Figure 1a). There is a second shallow kink at Ca_{16}^- , which is barely visible in the experimental results and is also apparent in our results. For zinc clusters, the calculated EA is comparable to those of the Ca clusters except for Zn_2^- , which yields a negative EA consistent with not being observed experimentally. The EA kink at Zn_{10} is similar to the one observed for the calcium clusters, with the exception that Zn_9^- is remarkably stable and therefore the kink seems shallower when compared to the calcium case. As is shown in Figure 4, the EA results are systematically lower than the experimental values for both Ca and Zn clusters. It is unfortunate that the experimental results do not carry error bars to allow for closer comparison. Zn_{10} and Zn_{11} are the two values of the EA with worst comparison to experiment, which might be evidence that other neutral isomers with lower ground-state energy exist but have not been found in this work nor in previous work.^{19,20}

Predictions from CC calculations¹⁸ reported Zn_3^- as unstable. However, this cluster anion has now been detected experimentally by two groups,^{8,17} and confirmed by our calculation. In ref 18 the reported EAs of Zn_4 , Zn_5 , and Zn_6 are lower than the experimental results⁸ by 0.22, 0.35, and 0.87 eV, respectively. The discrepancies of our results with the same experiment are 0.03, 0.07, and 0.35 eV, which are considerably smaller. The excellent qualitative agreement between our calculation and the experimental results of the EA is a validation of the methodology used in this work.

3. Excited States and Frequency Analysis of Ca_n ($n = 2$ –6) and Zn_n ($n = 3$ –6) Neutral and Anion Clusters

For the small Ca clusters containing two to six atoms, several excited states are identified for both anion and neutral clusters. As mentioned in section 2, these calculations were all done with the expanded basis set 6-311+G(d). Energies, symmetry, and state identification of the anions are reported in Table 3 along with the normal mode vibrational frequencies for all states. Table 4 contains results for the Ca neutral clusters. For Ca_2^- the ground state and three excited states are very close in energy.

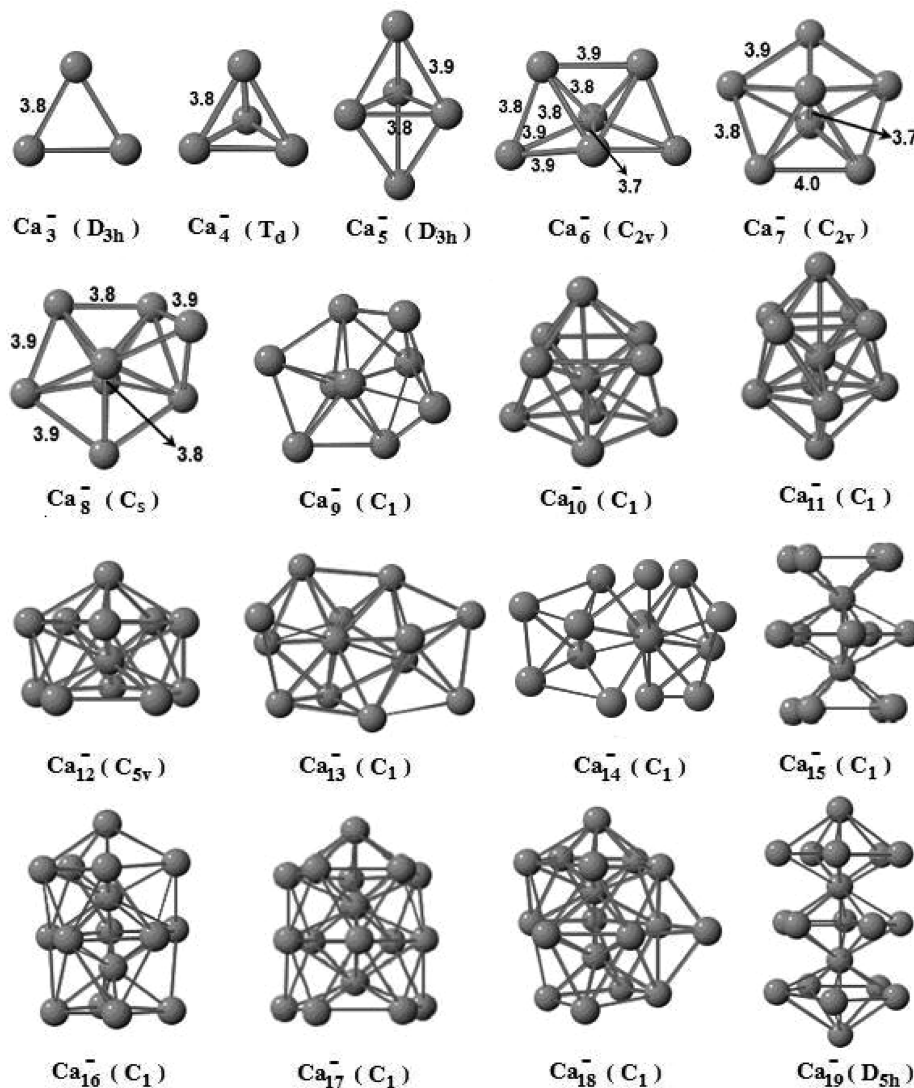


Figure 2. Structure of the calcium cluster anions. Bond lengths are rounded off and given in angstroms.

The bond length of this dimer anion in the ground state is 4.342 Å, which shrinks to 3.943 Å in the first excited state (doublet). In addition, two quartet excited states are identified for Ca₂⁻. For larger cluster anions Ca₃⁻ through Ca₆⁻, most of the excited states of the cluster anion maintain the ground-state geometry (Figure 2) with distortions responsible for the symmetry reduction. Ca₃⁻ D_{3h} has a bond length of 3.784 Å in the ground state and 3.968 Å in the first excited state. The Ca₃⁻ quartet excited state is an isosceles triangle with bond lengths 3.589/4.177 Å. The anion Ca₄⁻ T_d has bond length of 3.775 Å in the ground state, and its first quartet excited state D_{2d} is a distorted T_d structure with bond lengths 3.674/4.339 Å. The second quartet state C₁ corresponds to a Ca₄⁻ isomer with planar, almost rhomboidal, structure and bond lengths 3.876/3.693 Å. The Ca₅⁻ triangular bipyramidal structure with bond lengths 3.883/3.787 Å deforms in the excited states to have four different bond lengths: 3.838/3.955/3.747/3.577 Å in the doublet and 3.832/3.693/4.0/3.599 Å in the quartet. Similarly, Ca₆⁻ C_{2v} ground-state structure is shown in Figure 2 and the first and second excited states maintain the structure with some deformation. The second quartet excited state of Ca₆⁻ is a slightly deformed octahedron (C₁) with bond lengths 3.671/3.667/4.215/4.216 Å, which differs from the ground-state geometry.

Additionally, the singlet ground state, triple, and quintet excited states of neutral calcium clusters with n = 2–6 were calculated

and energy, symmetry, and state identification are reported in Table 4 (second through fourth columns). In this table, energies of the neutrals are relative to the ground-state energy of the corresponding size anion given in Table 1.

Similarly, for the small Zn clusters containing two to six atoms, several excited states are identified for both anion and neutral clusters. As for calcium, these calculations were done with the expanded basis set 6-311+G(d). Energies, symmetry, and state identification of the anions are reported in Table 5 along with the normal mode vibrational frequencies for all states and in Table 6 for the Zn neutral clusters. The anion ground-state structures are depicted in Figure 3. For Zn₃, the ground state and the first excited state are equilateral triangles D_{3h} and the second excited state is a quasi-linear C_{2v} structure. The bond length in the ground state is 2.695 Å, which elongates in the first excited state to 2.879 Å and shrinks to 2.393 Å in the quasi-linear excited state. Tetrahedral Zn₄⁻ bond length is 2.718 Å, which deforms into a planar square with edge 2.556 Å in the excited state. The triangular bipyramidal structure of Zn₅⁻ in the ground state has bond lengths 2.895/2.771 Å, which compresses to 2.727/2.696 Å in the excited state. Zn₆⁻ is a pentagonal pyramid with edges 2.802/2.705 Å, which deforms considerably in the first excited state (apex atom at 2.616 Å from vertices of an imperfect pentagon). The second excited state structure is composed of two distorted tetrahedra sharing one edge and bond

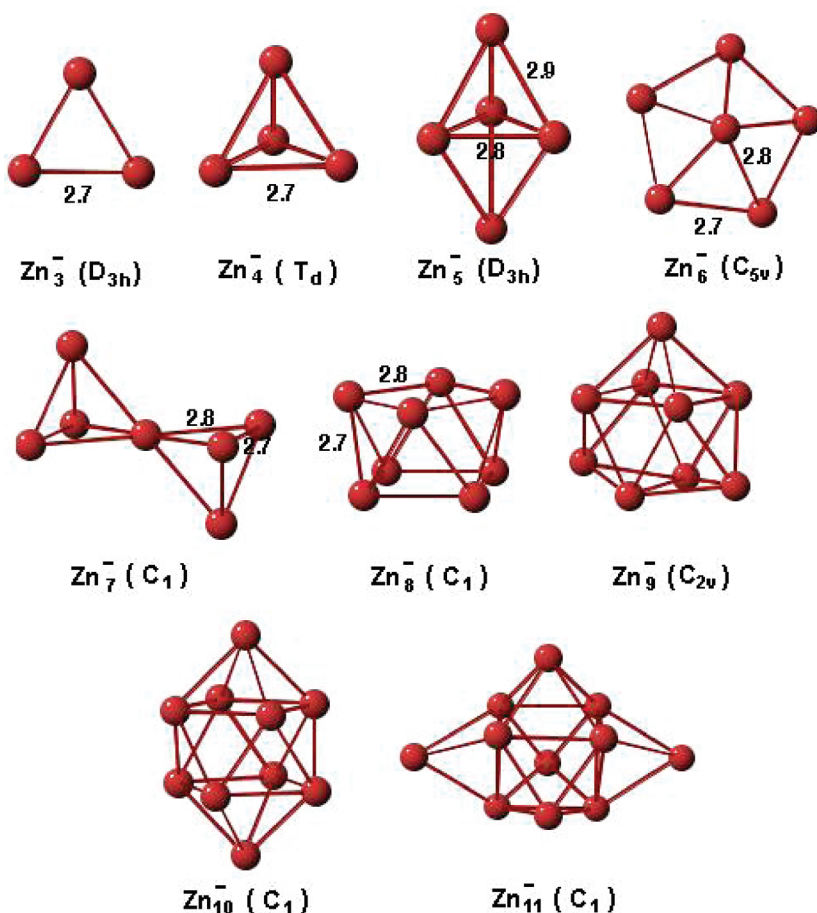


Figure 3. Structure of the zinc cluster anions. Bond lengths are rounded off and given in angstroms.

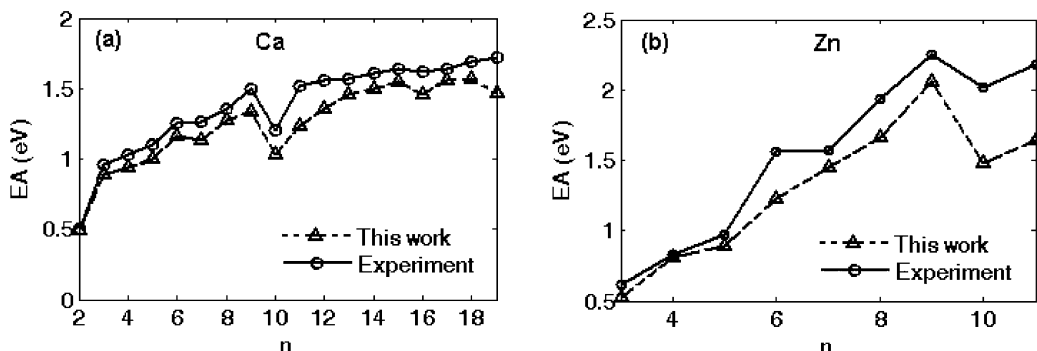


Figure 4. Electron affinity as a function of cluster size: (a) calcium; (b) zinc. Dotted lines correspond to this work and full lines to experiments in ref 8.

lengths spanning 2.680–3.065 Å. The quartet excited state of Zn_6^- is a deformed square pyramid with one atom decorating one of the triangular faces.

The singlet ground state, triplet, and quintet excited states of neutral zinc clusters with $n = 3\text{--}6$ are also studied. Energy, symmetry, and state identification are reported in Table 6 (second through fourth columns). As in the case of calcium, energies of these states are relative to the ground-state energy of the cluster anion of equal size reported in Table 2.

4. Electron Detachment Spectra of Cluster Anions Ca_n ($n = 2\text{--}6$) and Zn_n ($n = 2\text{--}6$)

Recent experiments on Ca and Zn cluster anions photoelectron detachment^{8,17} may yield experimental information about the structure of the neutral clusters by recording the kinetic energy

of the electron detached from the cluster anions. This energy is referred to by the experimental community as the electron binding energy (BE), which is the energy difference between the ground state of a cluster anion and the ground or excited states of the neutral cluster obtained when the electron is detached. Depending upon the experimental method, electrons might be detached if the anion is in a low-lying excited state. These low-lying excited states could be accessed in the experiment when the cluster anions are formed or the photo-photon are absorbed. Then, the electron detachment spectrum would contain a richer set of BEs, which would contribute to peak broadening or be a source of additional peaks. Experiments were carried out at about 3 eV photon energies for Ca and Zn^8 and close to 5 eV for Zn^{17} . In order to cover the experimental energy range, the ground state of the neutral and anion clusters

TABLE 3: Excited States of Ca_2^- through Ca_6^- and Their Vibrational Frequencies^a

| Ca_n^- | sym | state | E (eV) | frequency (cm^{-1}) |
|-----------------|----------------|----------------|----------|--|
| Ca_2^- | $D_{\infty h}$ | $^2\Sigma_g^+$ | 0.0 | 77 |
| | $D_{\infty h}$ | $^2\Pi_u$ | 0.0116 | 97 |
| | $D_{\infty h}$ | $^4\Sigma_u^+$ | 0.6249 | 159 |
| | $D_{\infty h}$ | $^4\Pi_g$ | 0.7184 | 143 |
| | D_{3h} | $^2A_2''$ | 0.0 | 105(2), 123 |
| | D_{3h} | $^2A_1'$ | 0.1027 | 73(2), 106 |
| Ca_3^- | C_{2v} | 4B_1 | 0.7032 | 56, 72, 144 |
| | T_d | 2A_1 | 0.0 | 86(2), 106(3), 134 |
| | D_{2d} | 4A_2 | 0.8914 | 51, 70, 98, 100, 103, 142 |
| Ca_4^- | C_1 | 4A | 0.9695 | 25, 61, 85, 115, 127, 135 |
| | D_{3h} | $^2A_1'$ | 0.0 | 62(2), 84, 85(2), 86, 94, 95, 139 |
| | C_{2v} | 2B_1 | 0.1439 | 53, 65, 72, 79, 90, 104, 132, 133, 152 |
| Ca_5^- | C_{2v} | 4B_1 | 0.4153 | 37, 59, 66, 79, 91, 107, 109, 135, 141 |
| | C_{2v} | 2A_2 | 0.0 | 46, 57, 61, 71, 82, 96, 102, 106, 112, 123, 127, 146 |
| | C_{2v} | 2A_1 | 0.0170 | 46, 58, 66, 85, 86, 93, 95, 98, 104, 113, 116, 150 |
| Ca_6^- | C_{2v} | 4B_1 | 0.3102 | 44, 55, 56, 64, 82, 87, 91, 100, 118, 136, 137, 146 |
| | C_1 | 4A | 0.4762 | 44, 49, 53, 61, 77, 81, 82, 84, 103, 109, 132, 132 |

^aEnergies (E) are relative to the ground state of the cluster anions reported in Table 1. The basis set 6-311+G(d) is used.

TABLE 4: Ground and Excited States of Ca_2 through Ca_6 and Electron Binding Energies BE^a

| Ca_n | sym | state | E (eV) | BE (eV) | | | |
|---------------|----------------|----------------|----------|----------------|-----------|----------------|-----------|
| | | | | $^2\Sigma_g^+$ | $^2\Pi_u$ | $^4\Sigma_u^+$ | $^4\Pi_g$ |
| Ca_2 | $D_{\infty h}$ | $^1\Sigma_g^+$ | 0.5124 | 0.5136 | 0.5286 | | |
| | $D_{\infty h}$ | $^3\Pi_u$ | 1.3848 | 1.7335 | 1.4984 | 0.7635 | 0.6954 |
| | $D_{\infty h}$ | $^3\Sigma_u^+$ | 1.4321 | 1.5422 | 1.4251 | 0.9500 | 0.7312 |
| | $D_{\infty h}$ | $^5\Sigma_u^+$ | 2.9172 | 3.4241 | 3.1827 | 2.3319 | 2.3443 |
| | $D_{\infty h}$ | $^5\Pi_u$ | 3.0139 | 3.1181 | 3.0140 | 2.4505 | 2.2979 |
| BE (eV) | | | | | | | |
| Ca_n | sym | state | E (eV) | $^2A_2''$ | $^2A_1'$ | 4B_1 | |
| Ca_3 | D_{3h} | $^1A_1'$ | 0.8891 | 0.9106 | 0.7880 | | |
| | C_{2v} | 3A_1 | 1.7620 | 1.8524 | 1.7667 | 1.0911 | |
| | C_{2v} | 5A_1 | 2.7466 | 2.7593 | 2.6692 | 2.0770 | |
| BE (eV) | | | | | | | |
| Ca_n | sym | state | E (eV) | 2A_1 | 4A_2 | 4A | |
| Ca_4 | T_d | 1A_1 | 0.9557 | 0.9559 | | | |
| | D_{2d} | 3B_2 | 1.7895 | 1.9093 | 0.9526 | 0.9872 | |
| | C_1 | 5A | 2.6871 | 3.0696 | 2.1355 | 1.7449 | |
| | C_2 | 5B | 2.8344 | 3.2322 | 2.3559 | 1.7451 | |
| BE (eV) | | | | | | | |
| Ca_n | sym | state | E (eV) | $^2A_1'$ | 2B_1 | 4B_1 | |
| Ca_5 | D_{3h} | $^1A_1'$ | 1.0084 | 1.0315 | 0.8964 | | |
| | C_1 | 3A | 1.4384 | 1.5308 | 1.4747 | 1.0707 | |
| | C_{4v} | 5A_2 | 2.3865 | 2.5926 | 2.5663 | 2.3292 | |
| BE (eV) | | | | | | | |
| Ca_n | sym | state | E (eV) | 2A_2 | 2A_1 | 4B_1 | 4A |
| Ca_6 | C_{2v} | 1A_1 | 1.1554 | 1.1719 | 1.1770 | | |
| | C_{2v} | 3B_1 | 1.4277 | 1.5023 | 1.5861 | 1.1697 | 1.3405 |
| | C_1 | 3A | 1.6164 | 1.5023 | 1.5431 | 1.1691 | 1.4648 |
| | C_{2v} | 5B_1 | 1.8498 | 2.0751 | 1.9763 | 1.6500 | 1.5349 |

^aNeutral clusters' energies (E) are relative to the ground state of the cluster anion in Table 1. Missing entries correspond to anion geometries not allowed in the state of the neutral clusters. The basis set 6-311+G(d) is used.

and their excited states laying within that energy window need to be calculated.

Presumably the electron detachment process is extremely fast, thus the ground state and the excited states of the neutral cluster are accessed experimentally at the same geometry of the anion.

This conjecture has been used repeatedly in the literature.^{30,31} However, we found that the energy of the neutral cluster in the geometry of the anion cluster might not belong to a point of the energy surface of any of the stable electronic states of the neutral cluster. This is a fundamental feature of two electronic states that cross in space; the intersection between the two surfaces is associated to only a few geometrical configurations. In this paper we report those cases where the energy surface of the neutral contains the point calculated at the frozen anion configuration, such that the BE is defined as:

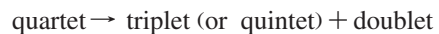
$$\text{BE} = E_n(\text{neutral at anion's frozen geometry}) -$$

$$E_n(\text{anion at equilibrium}) \quad (1)$$

This electron detachment mechanism can be viewed as a unimolecular reaction. For example, for calcium clusters:



The electron has spin $1/2$ (equivalent to a doublet), and the two elements considered in this work, Ca and Zn, have an even number of electrons. Thus, the reaction to detach an electron can proceed exclusively according to the spin angular momentum rules in the following combinations of state multiplicities:



Therefore, if the cluster anion is in a state with spin multiplicity 2, in order to detach one electron the singlet, triplet, and quintet states of the neutral cluster need to be taken into consideration. On the other hand, if the electron is detached from the cluster anion in a state with spin multiplicity 4, only triplet and quintet states of the neutral cluster need to be considered.

The predicted theoretical BEs using eq 1 and energy information in Tables 3–6 are reported in Tables 4 and 6. These BEs are calculated without considering the zero point energy of the cluster anion states. In fact, zero point energies are very small: 0.006, 0.021, 0.039, 0.049, and 0.07 eV for the ground states of Ca_2^- through Ca_6^- and 0.021, 0.038, 0.038, 0.062 eV for Zn_3^- through Zn_6^- . Missing values in Tables 4 and 6 indicate that the frozen configuration of the anion is not a point in the energy surface of the neutral cluster.

Figure 5 contains comparison between the calculated BEs reported in Table 4 for calcium cluster anions (dashed line and spikes) and the experimental results⁸ (continuous gray line).

TABLE 5: Excited States of Zn_3^- through Zn_6^- and Their Vibrational Frequencies^a

| Zn_n^- | sym | state | E (eV) | frequencies (cm^{-1}) |
|----------|----------|-----------|----------|--|
| Zn_3^- | D_{3h} | $^2A_1'$ | 0.0 | 104(2), 128 |
| | D_{3h} | $^2A_1'$ | 0.1670 | 67(2), 97 |
| | C_{2v} | 4B_1 | 1.5854 | 21, 151, 239 |
| Zn_4^- | T_d | 2A_1 | 0.0 | 87(2), 100(3), 135 |
| | C_1 | 4A | 1.4654 | 43, 59, 96, 126, 127, 162 |
| Zn_5^- | D_{3h} | $^2A_1'$ | 0.0 | 52(2), 58(3), 66(2), 90, 119 |
| | D_{3h} | $^4A_2''$ | 1.6792 | 30(2), 99(2), 120, 131(2), 136, 156 |
| Zn_6^- | C_{5v} | 2A_1 | 0.0 | 27(2), 59(2), 64, 79(2), 111, 113(2), 134(2) |
| | C_{2v} | 2A_1 | 0.0124 | 18, 33, 36, 37, 91, 94, 105(2), 107, 129, 147, 160 |
| | C_i | 2A_g | 0.1094 | 21, 33, 46, 54, 59, 75, 86, 96, 105, 109, 117, 128 |
| | C_1 | 4A | 1.0435 | 18, 21, 45, 47, 66, 83, 103, 108, 126, 143, 147, 179 |

^aEnergies (E) are relative to the ground state of the cluster anion given in Table 2. The basis set 6-311+G(d) is used.

TABLE 6: Ground and Excited States of Zn_3 through Zn_6 and Electron Binding Energies (BE)^a

| Zn_n | sym | state | E (eV) | BE (eV) | | | | |
|--------|----------|-----------|----------|----------|-----------|---------|--|--|
| | | | | $^2A_1'$ | $^2A_1'$ | 4B_1 | | |
| Zn_3 | D_{3h} | 1A_1 | 0.5265 | 0.6394 | 0.3771 | | | |
| | C_s | $^3A''$ | 2.3716 | 2.8805 | 2.8990 | 0.8044 | | |
| | D_{3h} | $^5A_2''$ | 4.7562 | 4.9051 | 5.0537 | 4.3706 | | |
| | | | | BE (eV) | | | | |
| Zn_4 | sym | state | E (eV) | 2A_1 | 4A | | | |
| | | | | 0.8077 | 0.8220 | | | |
| | | | C_1 | 3A | 3.3773 | 1.2022 | | |
| | | | | BE (eV) | | | | |
| Zn_5 | sym | state | E (eV) | $^2A_1'$ | $^4A_2''$ | | | |
| | | | D_{3h} | $^1A_1'$ | 0.8942 | 0.9684 | | |
| | | | C_1 | 3A | 2.2065 | 2.8948 | | |
| | | | | C_1 | 5A | 0.9441 | | |
| Zn_6 | sym | state | E (eV) | 2A_1 | 2A_1 | 2A_g | | |
| | | | C_{2v} | 1A_1 | 1.2242 | 1.5030 | | |
| | | | C_1 | 3A | 2.4626 | 2.7243 | | |
| | | | | C_1 | 3A | 2.5204 | | |
| | | | C_1 | 5A | 3.4881 | 4.4567 | | |
| | | | | 1.3102 | 2.8264 | 2.9674 | | |
| | | | | 1.2725 | 1.4862 | 1.4862 | | |
| | | | | 4.7607 | 4.8815 | 3.5895 | | |
| | | | | 4A | | | | |

^aNeutral cluster energies (E) are relative to the cluster anions' ground state in Table 2. Missing entries correspond to anion geometries not allowed in the state of the neutral clusters. The basis set 6-311+G(d) is used.

Although the experimental peaks are broad, across these cluster sizes there are three features that we identify as the electron detaching from the ground state of the cluster anion and accessing the singlet, triplet, and quintet states of the neutral cluster of equal size. Peak broadening of the three major BEs is expected because the cluster anion may be occupying a band of vibrational states when the electron is detached. Vibrations in the neutral cluster states are also expected to be excited. Therefore a vibrational broadening is added to each of the three major BEs using the vibrational frequencies reported in Table 3. Multiple excitations of vibrational states shift the BEs also reported in Table 4 by about 0.1 eV and give substantial broadening. The dotted line in Figure 5 shows the shape of the peak corresponding to BEs from the anion ground state to the ground and excited states of the neutral clusters when 10 vibrational states are used in the broadening. The height of the calculated peaks is scaled such that the calculated and experimental first peak intensity coincide and this scaling factor is

used for the rest of the calculated spectrum. Electrons detaching from excited states of the cluster anion are less abundant; BEs from these states contribute to broaden the three main peaks. These secondary BEs are reported in Table 4 and shown as delta functions in Figure 5. The tallest spikes correspond to BEs originated from the anion first exited state and spikes with decreasing height correspond to BEs from the second and third excited states of Ca_n^- .

The experimental gap between the first and the second peak can then be identified as the energy difference between the ground and first excited states of the neutral cluster. The calculated gaps are 0.95, 0.92, 1.28, 0.47, 0.32 eV for Ca_2^- through Ca_6^- , which are in very good agreement with the experimental values of 1.13, 0.81, 1.02, 0.55, and 0.47 eV, respectively. The major discrepancy is for Ca_4^- , where the experimental second peak shows a clear splitting, which gives rise to two energy gaps of 1.0 and 1.3 eV. Our calculation matches better the higher energy gap. A closer look at the experimental shape of the low-energy BE peak shows a systematic shoulder toward low energies for all clusters except Ca_4^- . This shoulder may be assigned to detachment from the first excited doublet of the anion to the ground state of the neutral cluster. As shown in Table 3, cluster anions of all sizes have a first excited state that is very close in energy to the ground state except for Ca_4^- . Therefore, this characteristic is another agreement between theory and experiment.

Other higher energy excited states of the neutral clusters may exist, but their study within the hybrid DFT is not adequate. Therefore, there are still unknowns for the full interpretation of the experimental BEs. Specifically, for Ca_5^- and Ca_6^- the experimental spectrum shows features at BEs greater than 2.5 eV, which may correspond to higher energy excited states. In the case of Ca_4^- there might be additional excited singlet states of neutral Ca_4 that we were unable to locate. Other geometries of Ca_4 were only found to be stable for a quintet excited state at a BE above 3.5 eV.

Following the same procedure as for calcium clusters, the electron detachment energy of Zn_n^- ($n = 3-6$) was theoretically predicted by calculating the energy difference between the states of the anions and the states of neutrals at the geometry of the anions. The gray continuous line in Figure 6 depicts the experimental results reported in ref 17 and the dashed line corresponds to the calculated BE between the ground state of the anion and the singlet, triplet, and quintet states of the neutral cluster. Worth noting is that the experimental results in ref 8 are almost identical to those of ref 17 and were obtained contemporarily. In our calculation, the BEs have been broadened considering a band of 10 vibrational states for each of the two electronic states involved according to frequencies reported in

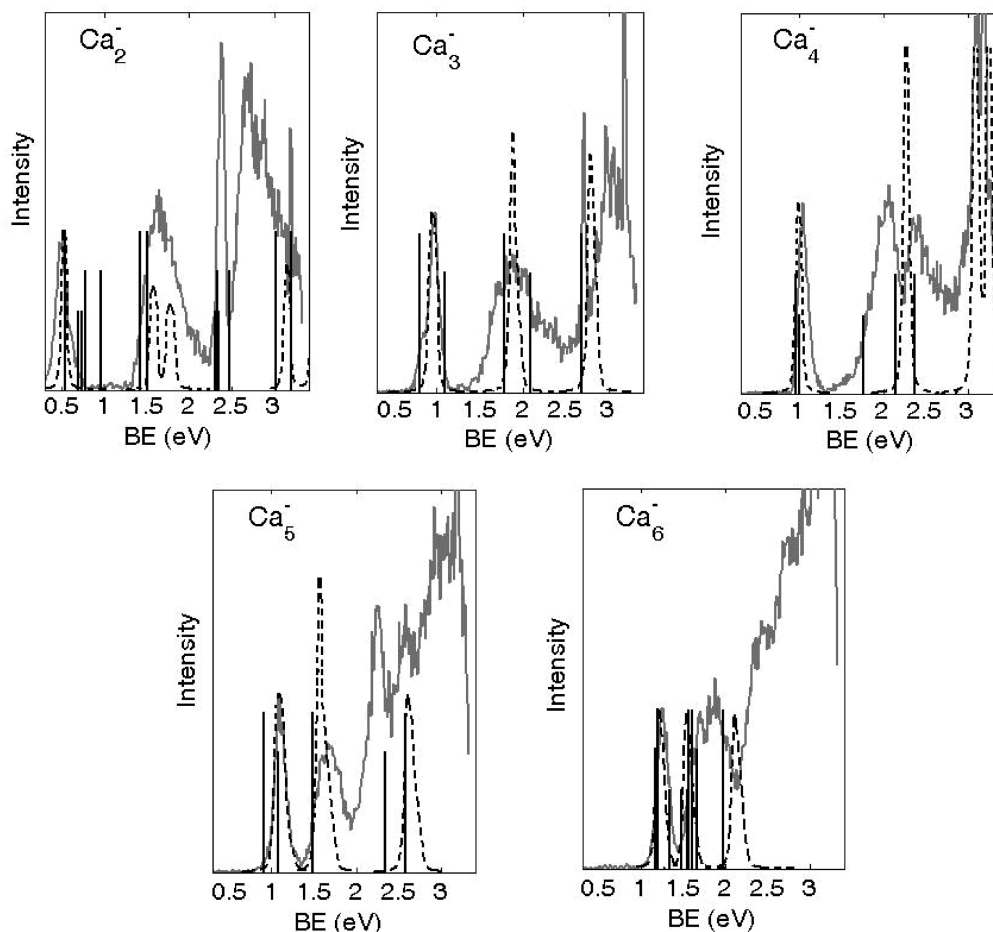


Figure 5. Electron binding energy of calcium cluster anions. Dotted lines are vibration-broaden calculated BEs from the ground state of the anion to the ground and excited states of the neutral. Spikes are calculated BEs from the excited states of the anion. The gray solid line is the experiment in ref 8.

Table 5. The intensity of the first peak is scaled to coincide with the experiment, and the same scaling factor is used throughout the spectrum. Additionally, the delta functions in Figure 6 correspond to BEs from anion ground state to excited states of the neutral and from excited states of the anion to all available states of the neutrals (see Table 6). The tallest spikes correspond to energy differences from the anion ground state and lines with decreasing height correspond to the first, second, and third excited states of Zn_n⁻.

The experimental energy gaps between the first peak and second peak are 2.25, 2.62, 2.19, and 1.50 eV for Zn₃⁻ through Zn₆⁻, respectively. The calculated gaps of 2.22, 2.50, 1.93, and 1.22 eV are in excellent agreement with experiment. Experimentally the first peak of Zn₃⁻ and Zn₆⁻ shows a noticeable shoulder at low energies, which is consistent with BEs from the low excited states of the anion clusters shown as spikes in Figure 6.

5. Conclusion

On the basis of the hybrid DFT calculations, this paper provides novel information on the ground-state energetics, symmetry, and vibrational analysis of anion calcium clusters up to Ca₁₉⁻ and on anion zinc clusters up to Zn₁₁⁻ which allows for calculation of the electron affinity in this cluster size range. Comparison of the electron affinity results with experiment is excellent, reproducing the intriguing kink observed at Ca₁₀ and Zn₁₀. For calcium, this kink occurs because Ca₁₀ is a magic

number for the neutral clusters⁴ whereas Ca₁₀⁻ is a fairly unstable cluster anion as shown in Figure 1a. The EA kink in zinc clusters is not as pronounced, pointing to a fairly stable Zn₁₀¹⁹ that does not qualify as a magic number and a fairly unstable cluster anion as shown in Figure 1b.

The DFT method used is limited to only provide precisely the excited states that have different multiplicity than the ground states. Therefore, the calculated electron detachment spectrum is a portion of the experimental observations. The electron detachment spectra of Ca₂⁻ through Ca₆⁻ and Zn₃⁻ through Zn₆⁻ were calculated and compared with Zheng's⁸ and Kostko's¹⁷ experimental observations. The major spectral characteristics are well calculated for these small clusters, as evidenced by the agreement with experiment. The spectral gaps between the first and second experimental features are in excellent agreement with the calculated counterparts. It is predicted that the electron detachment spectra originate from cluster anions in the ground state, but some BEs are broadened when detachment occurs from the first few anion excited states. A good agreement on the broadening is due to the contribution of the excited vibrational states. The paper contains the vibrational analysis for the anion states originating the spectral peaks and identifies that spectral peaks in the higher energy region are due to neutral clusters reached in triplet and quintet excited states. Since the reachable states of the neutral clusters have different multiplicities, the electron detachment process may be used as a spin switch if tailored accordingly.

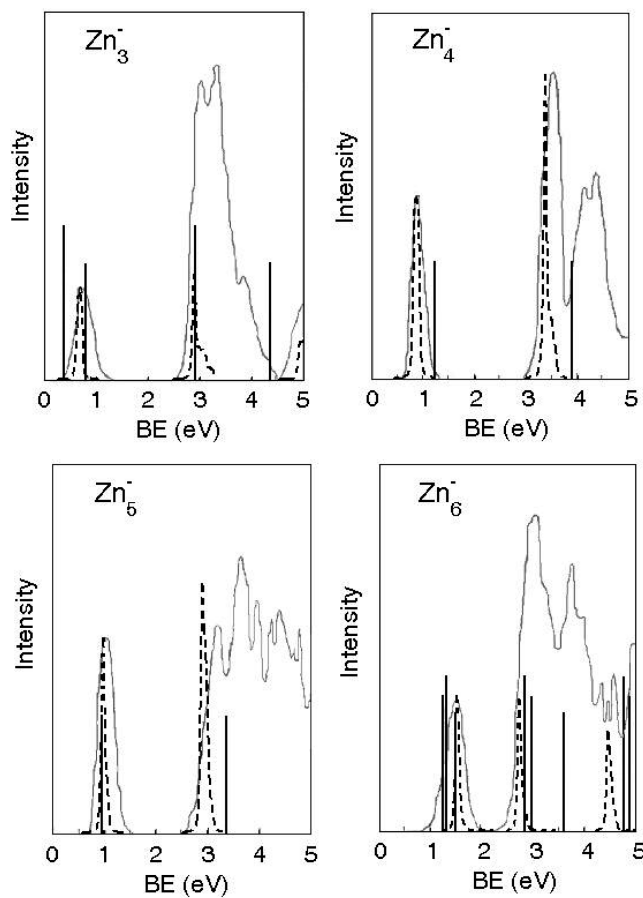


Figure 6. Electron binding energy of zinc cluster anions. Dotted lines are vibration-broaden calculated BEs from the ground state of the anion to the ground and excited states of the neutral. Spikes are calculated BEs from the excited states of the anion. The gray solid line is the experiment in ref 17.

Acknowledgment. We acknowledge the Teragrid Grant PHY050023T for approximately 10000 computational units used in this work and the George Mason University Provost Office for funding the research assistantship of Y.D. We are thankful to Professor Kit Bowen for calling our attention to the calcium and zinc electron detachment experiments in his group and for making available to us detailed files containing the experimental spectra.

References and Notes

- (1) De Heer, W. A. *Rev. Mod. Phys.* **1993**, *65*, 611.
- (2) Sugano, S.; Koizumi, H. *Microcluster Physics*; Springer-Verlag: New York, 1998.
- (3) For example, in: *Theory of Atomic and Molecular Clusters*; Jellinek, J. , Ed.; Springer-Verlag: New York, 1999.
- (4) Mirick, J. W.; Chien, C. H.; Blaisten-Baroja, E. *Phys. Rev. A* **2001**, *63*, 023202.
- (5) Dong, X.; Wang, G. M.; Blaisten-Baroja, E. *Phys. Rev. B* **2004**, *70*, 205409.
- (6) Blaisten-Baroja, E.; Chien, C. H.; Pederson, M. R.; Mirick, J. *Chem. Phys. Lett.* **2004**, *395*, 109.
- (7) Dong, X.; Blaisten-Baroja, E. *J. Comput. Theor. Nanosci.* **2006**, *3*, 118.
- (8) Zheng, W. Negative Ion Photoelectron Spectroscopy of Metal Clusters, Metal-organic Clusters, Metal Oxides, and Metal-doped Silicon Clusters. PhD Thesis(K. Bowen, Advisor). Johns Hopkins University: MD, 2005; Chapter 2.
- (9) Brechignac, C.; Broyer, M.; Cahuzac, Ph.; Delacretaz, G.; Labastie, P.; Wolf, J. P.; Woste, L *Phys. Rev. Lett.* **1988**, *60*, 275.
- (10) Kaiser, B.; Rademann, K. *Phys. Rev. Lett.* **1992**, *69*, 3204.
- (11) Rademann, K.; Dimopoulou-Rademann, O.; Schlauf, M.; Even, U.; Hensel, F. *Phys. Rev. Lett.* **1992**, *69*, 3208.
- (12) Busani, R.; Folker, M.; Cheshnovsky, O. *Phys. Rev. Lett.* **1998**, *81*, 3836.
- (13) Pastor, G. M.; Stampfli, P.; Bennemann, K. H. *Europhys. Lett.* **1988**, *7*, 419.
- (14) Moyano, G. E.; Wesendrup, R.; Sohn, T.; Schwerdtfeger, P. *Phys. Rev. Lett.* **2002**, *89*, 103401.
- (15) Garcia, M. E.; Pastor, G. M.; Bennemann, K. H. *Phys. Rev. B* **1993**, *48*, 8388.
- (16) Karakuse, I.; Ichihara, T.; Fujita, Y.; Matsuo, M.; Sakurai, T.; Matsuda, H *Int. J. Mass Spectrom. Ion Processes* **1986**, *69*, 109.
- (17) Kostko, O.; Wrigge, G.; Cheshnovsky, O.; Issendorff, B. V. *J. Chem. Phys.* **2005**, *123*, 221102.
- (18) Flad, H. J.; Schautz, F.; Wang, Y.; Dolg, M.; Savin, A *Eur. Phys. J. D* **1999**, *6*, 243.
- (19) Wang, J.; Wang, G.; Zhao, J. *Phys. Rev. A* **2003**, *68*, 013201.
- (20) Iokibe, K.; Tachikawa, H.; Azumi, K. *J. Phys. B* **2007**, *40*, 427.
- (21) McHugh, K. M.; Eaton, J. G.; Lee, G. H.; Sarkas, H. W.; Kidder, L. H.; Snodgrass, J. T. *J. Chem. Phys.* **1989**, *91*, 3792.
- (22) Liu, S-R; Zhai, H-J.; Castro, M.; Wang, L-S. *J. Chem. Phys.* **2003**, *118*, 2108.
- (23) Pramann, A.; Koyasu, K.; Nakajima, A.; Kaya, K. *J. Phys. Chem.* **2002**, *106*, 2483.
- (24) Perdew, J. P.; Chevary, J. A.; Vosko, S. H. i. e. *Phys. Rev. B* **1992**, *46*, 6671.
- (25) Perdew, J. P.; Burke, K.; Wang, Y. *Phys. Rev. B* **1996**, *54*, 16533.
- (26) Peng, C.; Ayala, P. Y.; Schlegel, H. B.; Frisch, M. J. *J. Comput. Chem.* **1996**, *17*, 49.
- (27) Ditchfield, R.; Hehre, W. J.; Pople, J. A. *J. Chem. Phys.* **1971**, *54*, 724.
- (28) Krishnan, R.; Binkley, J. S.; Seeger, R.; Pople, J. A. *J. Chem. Phys.* **1980**, *72*, 650.
- (29) Frisch, M. J.; et al. *Gaussian03*; Gaussian Inc.: Wallingford, CT, 1998.
- (30) Bonacic-Koutecky, V.; Fantucci, P.; Koutecky, J. *J. Chem. Phys.* **1990**, *93*, 3802.
- (31) Elliot, B. M.; Koyle, E.; Boldyrev, A. I.; Wang, X. B.; Wang, L. S. *J. Phys. Chem. A* **2005**, *109*, 11560.

JP8034067